DISCRETE-TIME *LQR* AND H_2 DAMPING CONTROL OF FLEXIBLE PAYLOADS USING A ROBOT MANIPULATOR WITH A WRIST-MOUNTED FORCE/TORQUE SENSOR

Chunhao Joseph Lee Constantinos Mavroidis
Robotics and Mechatronics Laboratory
Department of Mechanical and Aerospace Engineering
Rutgers University, The State University of New Jersey
98 Brett Road, Piscataway, NJ 08854-8058

ABSTRACT

This paper presents robust and optimal control methods to suppress vibrations of flexible payloads carried by robotic systems. A new improved estimator in discrete-time H_2 optimal control design based on the Kalman Filter predictor form is developed here. Two control design methods using state-space models, *LQR* and H_2 Optimal Design, in discrete-time domain are applied and compared. The manipulator joint encoders and the wrist-mounted six-degree-of-freedom force/torque sensor provide the control feedback. A complete dynamic model of the robot/payload system is taken into account to synthesize the controllers. Experimental verifications of both methods are performed using a Mitsubishi five-degree-of-freedom robot manipulator that carries a flexible beam. It is shown that both methods damp out the vibrations of the payload very effectively.

1. INTRODUCTION

Several industries in the modern world, such as manufacturing and space, require the execution of high speed and high accuracy tasks using robotic systems. In many cases, especially in the automotive, circuit board layout manufacturing plants or extra-vehicular activities in space environments, robots are needed to manipulate highly flexible and hence vibratory objects. Such payload vibrations decrease accuracy of the robotic system, create disturbances to the robot controller that may cause instabilities, and increase execution time of the whole operations since vibrations of the payloads have to be attenuated before any other task takes place. Therefore methods for damping the vibrations of the flexible payload carried by robotic systems need to be developed. These methods should use sensors and actuators placed on the robot rather then the payload since the payload is usually unknown, has various sizes and it will be very impractical and expensive to place different sensors and actuators on all payloads.

Methods to attenuate vibratory motions of flexible payloads in robotic systems have been studied. They can be distinguished into two main categories: passive and active damping control. Passive approaches consist of either planning the manipulator motion in advance to prevent the vibratory motion, or place mechanical dampers at the gripper of the manipulators to guarantee the performance [1]. The advantage of such methods is that the robot position and/or force control strategy does not interfere with the damping process. The disadvantages however are that the speeds are reduced, the trajectories are limited due to the design criteria, and the stability of the operations is not guaranteed.

Active control for damping vibrations of flexible manipulators and structures has been an active research area for a long time [2]-[5]. These control schemes could also be applied in systems that a rigid manipulator is handling a flexible payload. However, in these cases, it will be required to attach sensors, such as accelerometers and/or strain gauges, directly on the payload and thus the system and the applications lose their generality. Therefore, methods are needed for damping the payload vibrations using sensors external to the flexible payload.

An external optical camera was used by Alder and Rock to feedback the displacement and orientation of an unknown payload for an adaptive control framework [6]. The self-tuning regulator adaptive scheme was applied for system identification in order to tune the control gains a priori. While this method was shown to be effective, its disadvantage is that the optical sensor has to be mounted on another platform outside the robotic system. In unstructured environments such as space, it will be impractical and challenging to install and calibrate the optical sensor.

Jain and Khorrami applied a robot wrist-mounted force/torque sensor to feedback the response of flexible payloads in an adaptive control scheme [7]. This scheme has been applied without using an accurate payload and actuator dynamic model in controller design. The time-varying transfer function estimation, which is based on Fast Fourier Transform, of data from the force/torque sensor is performed at longer sampling period (10 msec. in [7]) to update the control gains while the system is controlled by shorter sampling period (5 msec. in [7]). The disadvantage is that on-line adaptation requires complicated calculations and a period at the beginning to sample the data.

Handling of flexible payloads has also been performed using two or more manipulators that form a closed system [8]-[10]. The vibrations of the payload are constrained by the closed loop kinematic chain formed by the manipulators and the payload. The disadvantages of such a method are the reduced workspace and the complexity of the system inverse kinematics.

This paper presents robust and optimal control methods to suppress vibrations of flexible payloads carried by robotic systems. A new improved estimator in discrete-time H_2 optimal control design based on the Kalman Filter predictor form is developed here. Two control design methods using state-space models, *LQR* and H_2 Optimal Design, in discrete-time domain are applied and compared. The manipulator joint encoders and the wrist-mounted six-degree-of-freedom force/torque sensor provide control feedback. A complete dynamic model of the robot/payload system is taken into account to synthesize the controllers. Experimental verifications of both methods are performed using a Mitsubishi five-degree-of-freedom robot manipulator that carries a flexible beam. It is shown that both methods damp out the vibrations of the payload very effectively.

2. DYNAMIC MODEL AND CONTROL DESCRIPTION

In this paper, it is assumed that a p degree-of-freedom robot manipulator is holding a flexible payload which is modeled with finite number of modes as shown in Figure 1. When the manipulator starts to move from an initial position to a final location where a task has been defined, vibrations of the payload will be excited and degrade the precision of the whole system under certain conditions such as high-speed trajectories or sudden decelerations.

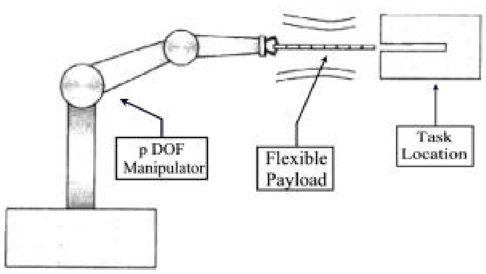

Figure 1: A Robot Manipulator Handles a Flexible Payload

Two types of sensors are used to feedback the system dynamic response. The encoders attached to the joint motors provide the manipulator joint position data, while the force/torque sensor placed at the manipulator wrist provides measurement of the force/moment interactions between the payload and the manipulator.

The goal of the active damping control is to keep the displacements of the flexible modes of the payload at zero all the time. If the damping controller is activated at the time that the manipulator end-effector has reached the final position and vibratory motion of the payload has to be attenuated, then the desired values for the positions of both the manipulator and the flexible payload can be initialized at zero so that the control problem becomes a regulation problem.

2.1. System Dynamic Model

The dynamic model in generalized state space form of the manipulator/payload system is needed in the controller synthesis. This model of the manipulator/payload and their interactions can be formulated by either Newton-Euler's or Lagrange's method [11]. The dynamic model is written into a global state space form as:

$$\begin{aligned} M_{inter}\ddot{x}_{inter} &= -D_{inter}\dot{x}_{inter} - K_{inter}x_{inter} + B_{inter}t_{ext} \\ &\quad - C_{inter}(x_{inter}, \dot{x}_{inter}) - G_{inter}(x_{inter}) \end{aligned} \tag{1}$$

$$M_{inter} = \begin{bmatrix} M + J^T M_{rigid} J & J^T a \\ a' & M_{flexible} \end{bmatrix},\ D_{inter} = \begin{bmatrix} 0 & 0 \\ 0 & D_{flexible} \end{bmatrix},$$

$$K_{inter} = \begin{bmatrix} 0 & 0 \\ 0 & K_{flexible} \end{bmatrix},\ B_{inter} = \begin{bmatrix} I_{p\times p} \\ 0_{6q\times p} \end{bmatrix}$$

where: $x_{inter} = \{q, v\}^T$ is a (*r´1*) vector (*r=p+6q*) includes both the joint angles q and flexible-mode vector v; the (*r´r*) matrices M_{inter}, D_{inter}, and K_{inter} are respectively the inertia, damping and stiffness matrices; the (*p´1*) vector t_{ext} represents the external inputs from the joint actuators; B_{inter} is the (*r´p*) coefficient matrix; the (*r´1*) vector C_{inter} represents the non-linear functions of Corriolis and centripetal forces; the (*r´1*) vector G_{inter} represents gravity forces. Inside the matrices listed above, M_{rigid} and $M_{flexible}$ are inertia matrices of manipulator and flexible payload; J is Jacobian Matrix from robot manipulator; a and a' are matrices describe the interactions between rigid body motion and the relative vibration modes.

2.2. Linearized Dynamic Model

The controller design methods require state space first-order ordinary differential equations. By treating all nonlinear terms in Equation (1) as external disturbances, the linearized state space equation can be written as:

$$\dot{x} = Ax + Bu \tag{2}$$

$$A = \begin{bmatrix} 0_{n\times n} & I_{n\times n} \\ -M_{inter}^{-1}K_{inter} & -M_{inter}^{-1}D_{inter} \end{bmatrix},\ B = \begin{bmatrix} 0_{n\times m} \\ -M_{inter}^{-1}B_{inter} \end{bmatrix}$$

where: $x = \{x_{inter}, \dot{x}_{inter}\}^T$ is the (*2r´1*) state space vector; $u = t$ is the (*p´1*) input vector; the (*m´1*) vector y represents output from sensors that provide information of the manipulator and payload motions (*m=p+6*).

The controller design requires the relation between the vector y and the state space vector x. The (*p´1*) vector y_1, the first part of the vector y, represents the manipulator joint angles which are measured directly from the joint encoders. The (*6´1*) vector y_2, the second part of the vector y, provides the information of vibration from the wrist-mounted force/torque sensor and is equal to the negative interaction forces/torques $t_{payload}$ expressed in the end-effector coordinate frame. By neglecting nonlinear terms (because they are considered disturbances), the linearized model equation is written as:

$$y = \begin{Bmatrix} y_1 \\ y_2 \end{Bmatrix} = Cx + Du \tag{3}$$

$$C = \begin{bmatrix} C_1 \\ C_2 \end{bmatrix},\ D = \begin{bmatrix} D_1 \\ D_2 \end{bmatrix}$$

$$C_1 = \begin{bmatrix} I_{p\times p} & 0_{p\times 6q} & 0_{p\times r} \end{bmatrix},$$

$$C_2 = -\begin{bmatrix} (J^T)^{-1}M + M_{rigid}J & a \end{bmatrix}\begin{bmatrix} A_{21} & A_{22} \end{bmatrix},\ D_1 = \begin{bmatrix} 0_{p\times p} \end{bmatrix},$$

$$D_2 = -\begin{bmatrix} (J^T)^{-1}M + M_{rigid}J & a \end{bmatrix}B_2$$

Since the manipulator/payload system is controlled by a computer which is treated as a discrete-time system, Equations (2) and (3) are discretized with a specified sampling period based on the zero-order-hold method described in [13] using the MATLAB command 'c2d.m'[14]. Hence, the state space model in discrete time domain has the form:

$$x_{n+1} = A_d x_n + B_d u_n,\ y_n = C_d x_n + D_d u_n \tag{4}$$

where n represents the current state and $n+1$ represents the state after the sampling period.

2.3. Discrete-Time Robust and Optimal Control Design

In this paper, the *Linear Quadratic Regulator* (*LQR*) [13] and the H_2 robust optimal control [15] design techniques will be used for damping the payload vibration. In this section, both methods are presented briefly. In addition, the new proposed discrete time Kalman estimator used in H_2 robust optimal control design is discussed in detail.

Both *LQR* and H_2 methods are using the separation theory to determine the state feedback control gain ($p \times 2r$) matrix K and estimator gain ($2r \times m$) matrix L independently. The discrete-time feedback control loop is shown in Figure 2 based on the dynamical system in Equation (4) and the actual system plant P.

At each time step n, the control input u is calculated based on the full state vector x_n and the control matrix K:

$$u_n = -Kx_n \tag{5}$$

Because the full state space vector x_n cannot be measured directly from the sensors, instead at each time step the estimated state space vector $\hat{x}_n$ is calculated using the measured data y and the estimator matrix L:

$$\hat{x}_{n+1} = A_d\hat{x}_n + B_d u_n + L(y_{n+1} - (C_d(A_d\hat{x}_n + B_d u_n) + D_d u_n)) \tag{6}$$

Thus the transfer function F of this feedback controller in discrete z domain is written as [15]:

$$F(z) = \left[\begin{array}{c|c} A_d - B_d K - LC_d A_d + LD_d K & L \\ \hline -K & 0 \end{array}\right] \tag{7}$$

In most of the cases, there are saturation limits for the input resources. The realization of the control algorithm using the Equations (5) and (6) is better than using the transfer function in Equation (7). The reason is that the estimated states are based on the saturated inputs rather than the designated 'unlimited' ones. The algorithm is shown in Figure 3.

2.3.1 Linear Quadratic Regulator and Kalman Estimator Method

Both *LQR* and *Kalman* estimator require optimization for which the Discrete-time Algebraic Ricatti equations are composed. The derivation is omitted due to the limit of the space. Full description can be found in [13]. If the system in Equation (4) (A_d,B_d) is controllable and the system (A_d,C_d) is observable, the design criterion for the best control gain K and observer gain L are set up accordingly:

$$J_K = \frac{1}{2}\sum_{n=0}^{N}\left(y_n^T Q y_n + u_n^T R u_n\right) \tag{8}$$

$$J_L = \sum_{n=0}^{\infty}\frac{1}{2}(y_n - C_d\hat{x}_n)^T W_n\,(y_n - C_d\hat{x}_n) \tag{9}$$

where both Q and R are weighting matrices; W_n is also a weighting matrix consisting with noise covariances. The boundary N for the summation is the stopping time step for the cost function, and most of the time it is set to approach infinity ($N \to \infty$). MATLAB has standard control tool box that helps to solve for both gains of K and L.

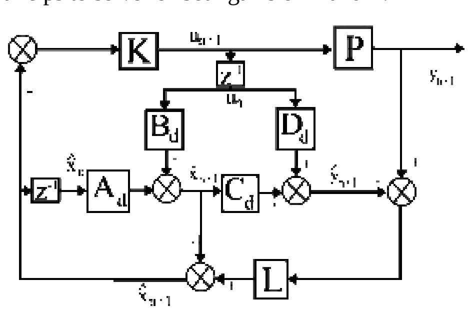

Figure 2: Discrete-Time *LQR/H₂* Control Loop

```
x_new = Ax+Bu+L*(y_new-C*(A*x+B*u)-D*u);
u_new = -K*x_new;
if (u_new > u_saturate) u = u_saturate;
elseif (u_new< - u_saturate) u = -u_saturate;
else u = u_new ;
x=x_new;
```

Figure 3: Algorithm for Computer Implemented *LQR/H₂* Control

2.3.2 H_2 Optimal Robust Control Design Method

While H_2 optimal robust control design in continuous time system has been used frequently, its implementation in discrete time systems has been given less attention. The implementation of H_2 control of discrete time system is presented in this subsection.

The robustness of the controller is determined by taking into account the disturbances of the system. The disturbances of inputs w_d and/or outputs v are weighted and integrated into the system of Equations (2) and (3) in continuous-time domain. The system is schematically presented in Figure 4, where W_u, W_{wd}, W_y, and W_v are user-defined weighting matrices; F is the controller designed by this method. The discrete time system is calculated using the MATLAB command 'c2d.m' and is written as:

$$x_{n+1} = A_d x_n + B_{d1}w_n + B_{d2}u_n\,,\;\; z_n = C_{d1}x_n + D_{d11}w_n + D_{d12}u_n\,,$$
$$y_n = C_{d2}x_n + D_{d21}w_n + D_{d22}u_n \tag{10}$$
$$w = \{w_d \quad v\}^T$$

where z is the output criterion defined by users and vector w represents all the weighted disturbances.

For H_2 optimal robust control method, the H_2 norm (norm in Hardy space) is used to form the cost function for optimization. The H_2 norm of Linear Time Invariant systems in discrete time domain is defined as [15]:

$$\|G(z)\|_2^2 = Trace\{D^*D + B^*L_oB\} = Trace\{DD^* + CL_cC^*\}$$

$$\text{for } G(z) = \left[\begin{array}{c|c} A & B \\ \hline C & D \end{array}\right] \in RH_2 \tag{11}$$

where L_o and L_c are the controllability and observability Gramians respectively.

Similarly to the *LQR/Kalman Estimator* method described in Section 2.3.1, the separation theory is applied so that optimal gains based on full-state feedback and optimal gains based on Kalman state estimation are calculated separately and then combined together without losing stability. Without losing generality, D_{22} is assumed zero since it can be recovered after the control gains are calculated [15]. The objective functions for both gain matrices K and L are formulated using the H_2 norm from disturbance w to state vector output z shown in Figure 5.

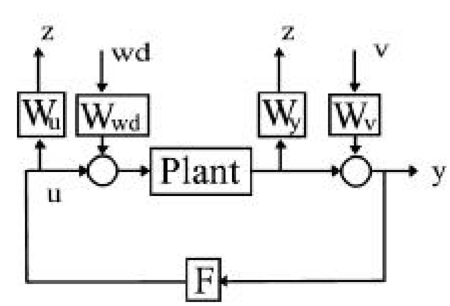

Figure 4: Feedback Loop with Weighting Consideration

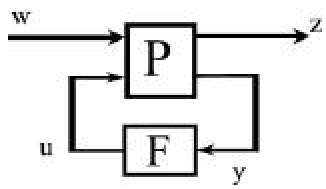

Figure 5: System Linear Fractional Transformation Representation [15]

In order to find the control gain matrix K of full-state feedback, the system matrices (A_d,B_{d2}) have to be controllable. The objective is to minimize the H_2 norm $\min_K \|T_{zw}\|_2^2$ from the following equations:

$$x_{n+1} = (A_d - B_{d2}K)x_n + B_{d1}w_n\,,\ z_n = (C_{d1} - D_{d12}K)x_n + D_{d11}w_n \quad (12)$$

$$T_{zw}(z) = \left[\begin{array}{c|c} A_d - B_{d2}K & B_{d1} \\ C_{d1} - D_{d12}K & D_{d11} \end{array}\right] \quad (13)$$

The corresponding Discrete-time Algebraic Ricatti Equation is

$$\begin{aligned} &A_K^T X_K A_K - X_K \\ &-\left(A_K^T X_K B_K + S_K\right)\left(B_K^T X_K B_K + R_K\right)^{-1}\left(B_K^T X_K A_K + S_K^T\right) + Q_K = 0 \\ &A_K = A_d\,,\ B_K = B_{d2}\,,\ S_K = C_{d1}^T D_{d12}\,,\ R_K = D_{d12}^T D_{d12}\,,\ Q_K = C_{d1}^T C_{d1} \end{aligned} \quad (14)$$

After solving for matrix X_K using the MATLAB command 'dare.m', the control gain matrix K is:

$$K = \left(B_{d2}^T X_K B_{d2} + D_{d12}^T D_{d12}\right)^{-1}\left(B_{d2}^T X_K A_d + D_{d12}^T C_{d1}\right) \quad (15)$$

Finding the gain matrix L, the method of Kalman Filtering is applied instead of the regular format described in [15]. If the system (A_d,C_{d2}) is observable, the system (A_d,$C_{d2}A_d$) is also observable thus the solution of the estimator is guaranteed [13]. Assuming that no external input applied, then Equation (10) becomes:

$$x_{n+1} = A_d x_n + B_{d1}w_n\,,\ y_n = C_{d2}x_n + D_{d21}w_n \quad (16)$$

The estimated states $\hat{x}_n$ are established as:

$$\begin{aligned} \hat{x}_{n+1} &= A_d\hat{x}_n + L(y_{n+1} - C_{d2}A_d\hat{x}_n) \\ &= A_d\hat{x}_n + L(C_{d2}A_d x_n + C_{d2}B_{d1}w_n + D_{d21}w_n - C_{d2}A_d\hat{x}_n) \end{aligned} \quad (17)$$

Then the error is set as:

$$e_n = x_n - \hat{x}_n$$

It has the Linear-Time-Invariant (LTI) form with the user-defined criterion variable z_n:

$$e_{n+1} = \left(A_d - LC_{d2}A_d\right)e_n + \left(B_{d1} - LC_{d2}B_{d1} - LD_{d21}\right)w_n\,,\ z_n = C_{d1}e_n$$

$$T_{zw}(z) = \left[\begin{array}{c|c} A_d - LC_{d2}A_d & B_{d1} - LC_{d2}B_{d1} - LD_{d2} \\ \hline C_{d1} & 0 \end{array}\right] \quad (18)$$

The design objective of the estimator gains is to minimize the H_2 norm $\min_L \|T_{zw}\|_2^2$. The associated Algebraic Ricatti Equation is:

$$\begin{aligned} &A_L^T X_L A_L - X_L \\ &-\left(A_L^T X_L B_L + S_L\right)\left(B_L^T X_L B_L + R_L\right)^{-1}\left(B_L^T X_L A_L + S_L^T\right) + Q_L = 0 \\ &A_L = A_d\,,\ B_L = \left(C_{d2}A_d\right)^T,\ S_L = B_{d1}\left(C_{d2}B_{d1} + D_{d21}\right)^T, \\ &R_L = \left(C_{d2}B_{d1} + D_{d21}\right)\left(C_{d2}B_{d1} + D_{d21}\right)^T,\ Q_L = B_{d1}B_{d1}^T \end{aligned} \quad (19)$$

After solving for matrix X_L, the gain matrix L is calculated as:

$$\begin{aligned} L = &\left(A_d X_L \left(A_d C_{d2}\right)^T + B_{d1}\left(C_{d2}B_{d1} + D_{d21}\right)^T\right) \\ &\cdot\left(\left(C_{d2}A_d\right) X_L \left(C_{d2}A_d\right)^T + \left(C_{d2}B_{d1} + D_{d21}\right)\left(C_{d2}B_{d1} + D_{d21}\right)^T\right)^{-1} \end{aligned} \quad (20)$$

3. EXPERIMENTAL PROCEDURES

3.1. Description of the Experimental System

The Dell® OptiPlex Gxa™ PC system with INTEL® Pentium II™ 333 MHz CPU and 128 MRAM is used in this work. It is augmented with two US Digital® PC7166™ PC to incremental encoder interface cards, two Datel® PC-412C™ Analog I/O boards and the force/torque sensor receiver that features an on-board digital signal processor (DSP). An amplifier was built with 6 high current, high power operational amplifiers Burr-Brown® OPA502. The PC collects the sensor readings either through the data acquisition boards, the encoder interface cards and the DSP receiver of force/torque sensor, does the feedback control calculation, and then sends out the signal to the actuators of the robotic systems through the D/A converter and laboratory built amplifiers.

A five-degree-of-freedom Mitsubishi RV-M2 manipulator is used in this research. Figure 6 shows schematically all mechanical and electrical components of this experimental system. The maximum payload capacity is 2kgf. The Mitsubishi manipulator is holding a thin aluminum beam that serves the purpose of a flexible payload. The beam is 0.610m long, 0.159m wide, 1.321×10^{-3}m thick, and is described in detail in Section 3.2.

A JR3® 67M25 6-axis force/torque sensor is placed at the manipulator wrist before the gripper as shown in Figure 6. It is capable of measuring a maximum force of 15lb in both x and y directions (shear forces) and 30lb in z direction (axial force) as well as a maximum torque of 39 in-lbs in all three directions. An Entran Accelerometer (Model EGE-732B-2000D-/RS), which is a strain gauge type sensor, is attached at the free-end of the flexible beam to record the oscillation and verify the relation between vibratory motion of the beam and data of the force/torque sensor. This sensor is used only for data acquisition purpose and not for the feedback signals of the controller in the experiment. WinRec v.1, a software developed in Robotics Laboratory, Rutgers University, provides deterministic fast timers based on MSDN library under Windows NT platforms. The timer in this experiment is set at 200Hz that is fast enough for the cut-off frequency to cover the first few modes of flexible specimen [18].

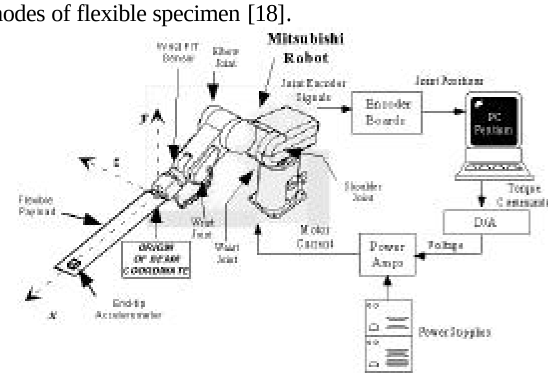

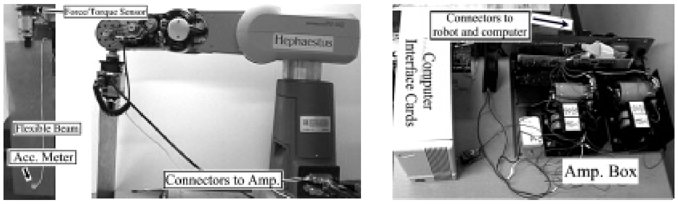

(a) the Beam (b) the Industrial Manipulator (c) the Signal Amp. and the Computer Interface

Figure 6: the Picture and Schematic of the Experimental System

3.2. Dynamic Model of the Flexible Beam

As it is described in Section 2.1, the dynamic model of the flexible beam in the end-effector coordinate frame is needed to be used in the control synthesis. The assumed modes method [11] is applied to form the dynamic model. For the derivation of the model, a long thin flat beam is considered, as it is shown in Figure 6, which has constant density m and vibrates only in the vertical direction. The displacement $v(x,t)$ of the flexible beam in the vertical direction is a function of both the longitudinal distance x and time t. Based on the theory of separation of variables, v can be written as:

$$v(x,t) = \sum_{l=1}^{n} j_l(x) q_l(t) \tag{21}$$

where $j_l(x)$ are the mode shape normal functions, $q_l(t)$ are the amplitudes and n is the number of vibratory modes. Thus, when one-degree joint actuation is used, the dynamic model of the beam, whose longitudinal length is L and cross-section area is A, can be written in the following form:

$$t_z = I_{zz}\dot{w}_z + a^T \ddot{q} + t_{dis} \tag{22}$$

$$t_z j'(0) - a\dot{w}_z = M\ddot{q} + D\dot{q} + Kq + t'_{dis} \tag{23}$$

where:

elements of M: $m_{kl} = \int_0^L mAj_k(x) j_l(x)dx$, both k and l are the number of the flexible mode;

elements of K: $k_{kl} = \int_0^L [EI_z j_k''(x) j_l''(x) + P(x) j_k'(x) j_l'(x)]dx$, E is Young's Modulus of the material; I_z is the cross-section area moment of inertia; P is the internal forces of the beam;

elements of a: $a_l = \int_0^L mAxj_l(x)dx$;

The damping coefficient D of the vibratory modes can be determined by the experimental data from the impulse disturbance at the free tip end;

w_z is the angular velocity along the z direction in Figure 6; I_{zz} is the sum of the second moment of inertia of the beam, the force/torque sensor and the gripper in z direction; t_z is the torque applied onto the beam the force/torque sensor and the gripper; both t_{dis} and t'_{dis} are the non-linear forces that are described as disturbances.

The characteristic equation of j_k, with the fix-end boundary conditions, and its partial derivatives are [11]:

$$f_k(x) = \sinh(b_k)\sin(\frac{b_k x}{L}) + \sin(b_k)\sinh(\frac{b_k x}{L}) \tag{24}$$

$$f_k'(x) = \frac{b_k}{L}\sinh(b_k)\cos(\frac{b_k x}{L}) + \frac{b_k}{L}\sin(b_k)\cosh(\frac{b_k x}{L}) \tag{25}$$

where b_k is the solution of the function: $\cos(b_n)\cosh(b_n) + 1 = 0$.

In order to simplify the experimental procedure, only one out of the manipulator 5 DC servomotors is used to damp the payload vibrations (see also Section 3.3). With this simplification, the manipulator dynamic model becomes the motor dynamic model. Under the assumption that the motor inductance is negligible compared to the motor resistance R, the relation between the motor torque t and the DC-voltage V is written as [12]:

$$t = h(K_i(\frac{V - K_m h\dot{q}}{R}) - B_m h\dot{q} - I_m h\ddot{q}) \tag{26}$$

where I_m is moment of inertia of the shaft, K_m is constant of back emf ; K_i is the torque constant; parameter h is the gear ratio of the motor.

The dimensions and density of the flexible beam are shown in Table 1. The mass moments of inertia in all three directions with respect both to the center of mass and the manipulator end-effector are shown in Table 2. Table 3 shows the moments of inertia of the other components attached between the beam and the motor. The motor characteristics are shown in Table 4. The damping ratio of the first-mode has been determined experimentally as $x = 0.045$ (see Section 4.1). The beam's natural frequencies W (Hz) for the first four-modes have been calculated and are shown in Table 5.

Table 1: Characteristics of the Aluminum Beam

Density	Weight	Length in x	Length in y	Length in z
2.8×10^3 Kg/m^3	0.358 Kg	0.6096 m	1.321×10^3 m	0.1588 m

Table 2: Mass Moments of Inertia (Kg-m2) of the Beam

Mass Mom. of Inertia	I_{xx}	I_{yy}	I_{zz}
About Center of Mass	7.52×10^{-4}	0.0118	0.0111
about the Fixed End	7.52×10^{-4}	0.0118	0.226

Table 3: Mass Moments of Inertia (Kg-m2) of Components

Force Sensor	Gripper
1.14×10^{-3}	0.0132

Table 4: Properties of the Motor

Torque Const. (Kg-m/A)	4.1×10^{-4}
Volt. Const. (V/(rad/sec.))	0.0401
Resist.(Ω)	3.4
Rotor Inertia (Kg*m/(rad/sec.))	4.3×10^{-7}
Static Fric. Torque(Kg-m)	1.2×10^{-3}
Gear Ratio	110
Amplifier gains	4.32

Table 5: First 4 Calculated Natural Frequencies

1st Mode (Hz)	2nd Mode (Hz)	3rd Mode (Hz)	4th Mode (Hz)
2.912	18.249	51.097	100.130

The system state space model takes a form equivalent to Equation (2):

$$\dot{x} = Ax + Bu\ ,\ A = \begin{bmatrix} 0_{n+1\times n+1} & I_{n+1\times n+1} \\ -M_{inter}^{-1}K_{inter} & -M_{inter}^{-1}D_{inter} \end{bmatrix},\ B = \begin{bmatrix} 0_{n+1\times 1} \\ -M_{inter}^{-1}B_{inter} \end{bmatrix}$$

$$M_{inter} = \begin{bmatrix} I_{zz} + h^2 I_m + I_{ext} & \{a\}^T \\ \{a\} & [M] \end{bmatrix},\ C_{inter} = \begin{bmatrix} -h^2(B_m + \frac{K_i K_m}{R}) & 0_{1\times n} & \\ 0 & -c_1 & 0_{1\times n-1} \\ & 0_{n-1\times n+1} & \end{bmatrix},$$

$$K_{inter} = \begin{bmatrix} 0 & 0_{1\times n} \\ 0_{n\times 1} & -[K] \end{bmatrix},\ B_{inter} = \begin{Bmatrix} 1 \\ j\,' \end{Bmatrix} h\frac{K_i}{R} \tag{27}$$

where $x = \begin{bmatrix} x_{inter} & \dot{x}_{inter} \end{bmatrix}^T$; $x_{inter} = \begin{bmatrix} q_z & q^T \end{bmatrix}^T$; and u is the voltage V.

The system measured outputs are the rotational angle q_z from the encoder of the manipulator pitch wrist motor and the reaction torque $t_{payload}$ from the force/wrist sensor. Hence, the output vector $y = \{q_z \quad t_{payload}\}^T$ is written as:

$$y = Cx + Du\ ,\ C = \begin{bmatrix} C_1 \\ C_2 \end{bmatrix},\ D = \begin{bmatrix} D_1 \\ D_2 \end{bmatrix}$$

$$C_1 = \{1 \quad 0_{1\times n}\},\ C_2 = -\begin{bmatrix} I_{zz} + I_{ext} & \{a\}^T \end{bmatrix} \begin{bmatrix} A_{21} & A_{22} \end{bmatrix},\ D_1 = 0\ ,$$

$$D_2 = -\begin{bmatrix} I_{zz} + I_{ext} & \{a\}^T \end{bmatrix} B_2 \tag{28}$$

3.3. Several Experimental Conditions

Only the first mode of the payload vibration is taken into account in the controller design because it has the most significant effect in the payload motion. Since the payload vibrations are in one direction and the goal is to attenuate the first mode, only one of the 5 manipulator motors will be used. This also simplifies the experiments without losing generality. The motor used is the one in the pitch of the wrist (Sanyo Denki® model R-402) and has rated armature voltage of 23 volt and peak maximum torque of 4.3 kgf-cm.

Static friction of the motor exists and cannot be neglected. Therefore a very simple friction compensation algorithm is needed. Since the direction of the friction is the same as that of the motor velocity which is the second element of the estimated state variables in Equation (27), a constant voltage equal to 0.5 volt is opposed following the direction of the velocity [17]. This value has been determined experimentally for the robot wrist motor.

The weighting parameters needed in *LQR* and H_2 controllers syntheses are chosen using trial and error methods. The weighting filters needed in H_2 are chosen as all-pass (constants).

4. RESULTS FROM CONTROL EXPERIMENTS

In the experiments of this research, the wrist joint moves the beam from initial horizontal position to final vertical position using joint PD control as shown in Figure 7. This 40° angular motion is performed in 0.3 second. The vibration is excited due to the fast start and stop of the motion. Once the final position is reached, either *LQR* or H_2 controller is switched on to damp the payload vibrations.

4.1. PD Joint Control without Damping Control

A set of experiments has been performed without any damping controllers to demonstrate the high amplitude and long settling time of the payload vibrations. A representative response is shown in Figure 8. The dashed line represents the torque measurement in z direction from the wrist-mounted force/torque sensor and the solid line represents the measurement of the free-end position of the flexible beam using double integration of the data from the accelerometer.

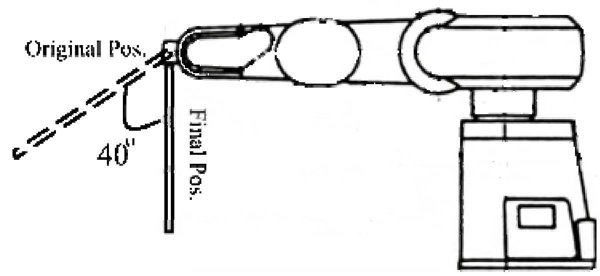

Figure 7: the Angular Motion of the Flexible Payload

From these data it can be determined that the under-damped frequency of the first mode from the experimental data is 2.55Hz, 15% off from the calculated natural frequency shown in Table 5. Both force/torque sensor and accelerometer data show a settling time of approximately 2.18 seconds (Note: In this paper, the settling time is defined as the time interval between the beginning of vibrations and the time instant that the vibrations are within 25% of the highest magnitude).

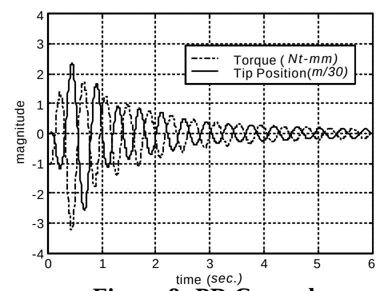

Figure 8: PD Control

4.2. *LQR/Kalman* Damping Control Method

The weighting matrices Q and R in control gain K, and the disturbance covariances $B_w^T R_{wp} B_w$ and R_{wm} in observer gain L have been chosen to be equal to:

$$Q = \begin{bmatrix} 10^5 & 0 \\ 0 & 2\times 10^4 \end{bmatrix},\ R = 3.2,\ B_w^T R_{wp} B_w = \begin{bmatrix} 1 & 0 \\ 0 & 1 \end{bmatrix},\ R_v = \begin{bmatrix} 10^6 & 0 & 0 & 0 \\ 0 & 3\times 10^6 & 0 & 0 \\ 0 & 0 & 1.5\times 10^6 & 0 \\ 0 & 0 & 0 & 2\times 10^6 \end{bmatrix}$$

The calculated gain matrices are:

$$K = \begin{bmatrix} 150.2883 & -1.092580\times 10^4 & 38.76203 & -78.30190 \end{bmatrix},\ L = \begin{bmatrix} 1.001055 & -1.084389\times 10^{-5} \\ -2.276218\times 10^{-3} & 3.312610\times 10^{-3} \\ 0.2096913 & -3.938525\times 10^{-3} \\ 0.3414154 & 4.132174\times 10^{-3} \end{bmatrix}$$

Results from the *LQR* damping control experiments are shown in Figure 9. It is clearly seen that the vibration setting time drops to 1.51 seconds, which is 69% of that with no damping control. Figure 10 shows a comparison between the experimental data from the joint motor encoder and from the force/torque sensor and the corresponding estimates using the Kalman estimator, which are almost identical. It is seen that the Kalman estimator calculated very accurately the state space vector. Also shown in Figure 10 is the control input.

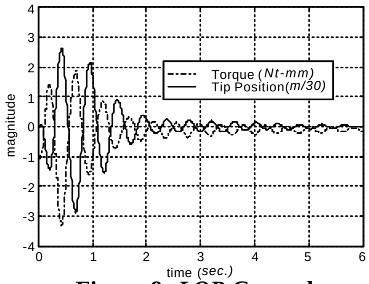

Figure 9: *LQR* Control

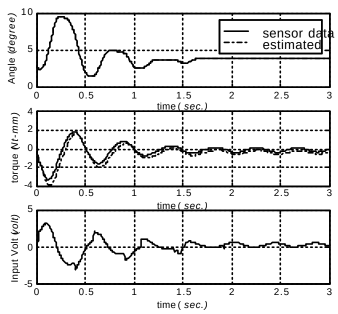

Figure 10: Input voltage and Outputs from Encoder and Force Sensor with *LQR* Controller

4.3. H_2 Damping Control Method

The values for the weightings and the control and estimator gains K and L are:

W_m	W_b	W_e	W_f	W_{ze}	W_{zf}	W_u
900	800	0.3	1.2	3.5×10^3	1.75×10^3	35

$$K = [93.09737 \quad -5282.966 \quad 31.21973 \quad -47.30177], \quad L = \begin{bmatrix} 0.2996878 & 5.292280\times10^{-4} \\ -0.1114448 & -1.544166\times10^{-3} \\ 10.92155 & -0.07311073 \\ -1.442574 & -0.1994574 \end{bmatrix}$$

The displacement of the flexible beam tip and the direct measurement of the force/torque sensor are shown in Figure 11 when H_2 damping control is used. The settling time is 1.18 sec., which is 54% of that with no damping control, and is less than the *LQR* method. The comparisons between the experimental data of the joint motor encoder and force sensor and the estimates with the Kalman estimator are shown in Figure 12. As with the *LQR* method, the estimates are very good. Figure 12 also shows the control input.

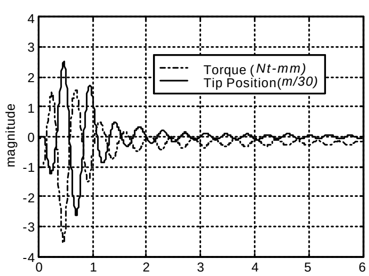

Figure 11: The Experiment with H_2 Controller

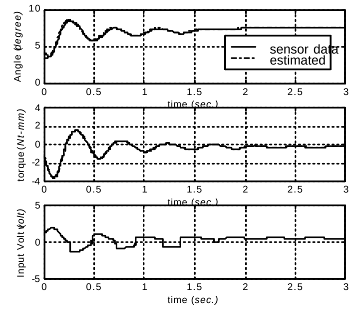

Figure 12: Input voltage and Outputs from Encoder and Force Sensor with H2 Controller

4.4. Robustness of *LQR* and H_2 Controllers

In order to test the robustness of the controllers, three different weights, 30*g* (8.4% of the original beam weight,) 60*g* (16.8%) and 100*g* (28%) are attached at the free-end of the flexible beam thus changing the dynamic properties of the system. Changes of the frequencies of the first mode of the beam are listed in Table 6. The comparisons of the different controllers are shown in Figure 13, Figure 14 and Figure 15. Table 7 lists the settling times as defined in Section 4.2. Both *LQR* and H_2 controllers have good performances when no extra weight was attached at the beam. With 8.4% increase of the weight both controllers still provide good results; but the performance of the *LQR* controller degrades with 16.8% increase of the weight. With 28% change of the weight, *LQR* is still stable but requires even more time then the controller without force feedback to damp out, while H_2 controller still has a good performance. Therefore the H_2 design shows superior robustness because the method takes into account the effects of the unstructured disturbances (uncertainty).

5. CONCLUSIONS

In this paper, the discrete-time *LQR* and H_2 control synthesis methods with a new scheme for the observer have been applied to damp the vibrations of payloads handled by rigid manipulators. The manipulator joint encoders and a wrist-mounted six-degree-of-freedom force/torque sensor provided the control feedback. The real-time control experiments at 200Hz sampling rate with a single joint of an industrial manipulator handling a flexible beam demonstrated good performances for both controllers. The controller designed using the H_2 method showed very good performance in robustness tests. In the future, the same observer scheme will be integrated into a robust/optimal discrete-time $H_¥$ controller.

6. ACKNOWLEDGMENTS

Chunhao Joseph Lee was supported by a Teaching Assistantship from the Department of Mechanical and Aerospace Engineering of Rutgers University. The authors would like to thank Professor Zoran Gajic from the Department of Electrical and Computer Engineering at Rutgers University, for his advise on control theories.

Table 6: Frequencies of the Beam with Weights

Without W	W = 30 g	W = 60 g	W = 100 g
2.55*Hz*	2.34*Hz*	2.09*Hz*	1.95*Hz*

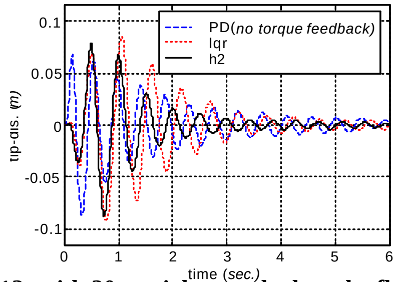

Figure 13: with 30g weight attached on the flexible beam

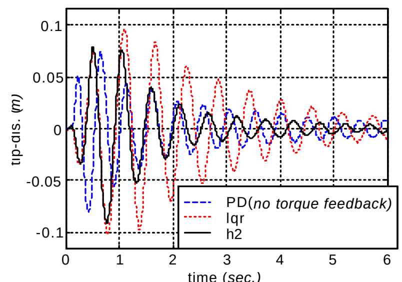

Figure 14: with 60g weight attached on the flexible beam

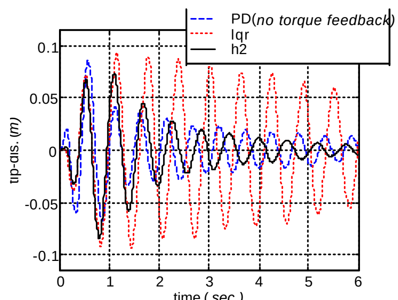

Figure 15: with 100g weight attached on the flexible beam

Table 7: Settling Times of 75% Vibration Attenuations

(sec.)	No Extra W	W = 30 g	W = 60 g	W = 100 g
PD Control (w/out force feedback)	2.18	2.79	3.45	4.54
LQR Control	1.51	2.47	4.05	>6.0
H_2 Control	1.18	1.57	2.15	2.58

7 REFERENCES

[1] Chen, M. Z. and Zheng, Y. F., 1995, "Vibration-Free Handling of Deformable Beams by Robot End-Effectors", *Journal of Robotic Systems*, 12(5), 331-347.

[2] Rovner, D. and Cannon, R. H. Jr., 1988, "Experiments Toward On-Line Identification and Control of a Very Flexible One-Link Manipulator", *The International Journal of Robotics Research*, 6(4), 3-19.

[3] Coffignal, G. Verge, M. Frikha, S. and Thourot, M., 1997, "Active Control of Structures: an Example of a Simple Experimental Set Up", *Proceedings of the International Modal Analysis Conference - IMAC. 2,* Bethel, CT, USA, 1987-1993.

[4] Meirovich, L. and Lim, S., 1994, "Maneuvering and Control of Flexible Space Robots", *Journal of Guidance Control and Dynamics*, ASME, 17(3), 520-528.

[5] Brogliato, B. Rey, D. Pastore, A. and Barnier J., 1998, "Experimental Comparison of Nonlinear Controllers for Flexible Joint Manipulators", *The International Journal of Robotics Research*, 17(3), 260-281.

[6] Alder, L. J. and Rock, S. M., 1994, "Experiments in Control of a Flexible-Link Robotic Manipulator with Unknown Payload Dynamics: an Adaptive Approach", *The International Journal of Robotics Research*, 13(6), 481-495.

[7] Jain, S. and Khorrami, F., 1995, "Positioning of Unknown Flexible Payloads for Robotic Arms Using a Wrist-Mounted Force/Torque Sensor", *IEEE Transactions on Control Systems Technology*, 3(2), 189-201.

[8] Nakagaki, H. Kitagaki, K. Tsukune, H., 1995, "Study of Insertion Task of a Flexible Beam into a Hole", *Proceedings of the 1995 IEEE International Conference on Robotics and Automation*, Nagoya, Japan, v1, 330-335.

[9] Yukawa, T., Uchiyama, M., Nenchev, D. N. and Inooka, H., 1996, "Stability of Control System in Handling of a Flexible Object by Rigid Arm Robots", *Proceedings of the 1996 IEEE International Conference on Robotics and Automation*, Minneapolis, MN, 2332-2339.

[10] Sun, D. Mills, J. K. and Liu, Y., 1999, "Position Control of Robot Manipulators Manipulating a Flexible Payload", *The International Journal of Robotics Research*, 18(3), 319-332.

[11] Baruh, H., 1999, *Analytical Dynamics*, WCB/McGraw-Hill.

[12] Craig, J. J., 1989, *Introduction to Robotics, Mechanics and Control*, 2nd Ed., Addison-Wesley.

[13] Franklin, G. F. Powell, J. D. and Workman, M., 1998, *Digital Control of Dynamic Systems*, 3rd Ed., Addison Wesley Longman.

[14] The Mathworks Inc., 1998, *Control System Toolbox, for Use with MATLAB-User's Guide*, v.4.1, Natick, MA.

[15] Zhou, K. Doyle, J. C. and Glover, K., 1996, *Robust and Optimal Control*, Prentice-Hall Inc.

[16] Grewal, M. S. and Andrews, A. P., 1993, *Kalman Filtering, Theory and Practice*, Prentice-Hall Inc.

[17] Amin, J. Friedland, B. and Harnoy, A., 1997, "Implementation of a Friction Estimation and Compensation Technique", *IEEE Control Systems*, 71-76, August.

[18] Lee, C. J. and Mavroidis, C., 1999, "PC Based Control of Robotic and Mechatronic Systems under MS-Window NT Workstation", *IEEE/ASME Transactions on Mechatronics*, submitted.